Kinetic Analysis of ZnO Filled PVA-LiCl: Three Phase Electrolyte

Abdullah F. M. Al Naim

Physics Department, Faculty of Science, King Faisal University
Al-Hassa, Saudi Arabia

ABSTRACT

A non-isothermal kinetics analysis for poly (vinyl alcohol) (PVA) and its ZnO nanocomposite (5wt.%) loaded with different weight ratios of LiCl, was investigated by thermogravimetric analysis (TGA). The degradation mechanism and the corresponding activation energies were calculated using Kissinger, Flynn-Wall-Ozawa and Coats-Redfern models at different heating rates (5, 10, 20, 30, 40, and 50 °C/min). In general, all models demonstrated their reliability to describe the thermal degradation of samples. The results show a reduction in PVA thermal stability in the presence of ZnO nanoparticles in the PVA matrix. Additionally, ZnO nanoparticles induce an alternative degradation mechanism from one-dimensional diffusion to random nucleation with one or two nuclei on the individual particles. However, the presence of the LiCl salt exhibits negligible effects on the TGA profiles and the activation energy values.

Key Words: Poly (vinyl alcohol), Thermal degradation, Thermal stability, ZnO nanoparticles.

INTRODUCTION

Hybrid materials composed of organic-inorganic constituents have received a wealth of interest, since the addition of inorganic nanoparticles to organic polymers can enhance their electrical, optical, and mechanical properties, in addition to improving catalytic activity (Godovsky 2000). Such methodologies are significant strategies to tailor new hybrid materials that combine the advantages of both constituents. Numerous applications were developed successfully in areas such as sensors, organic batteries, and microelectronics. Therefore, elucidating the thermal degradation properties of such hybrid composites are of current interest. Among various host polymers, poly(vinyl alcohol) (PVA) has demonstrated potential as a result of favorable chemical stability, encouraging mechanical, and thermal properties (Krumova *et al.*, 2000; Jin *et al.*, 2007) in addition to biodegradable, nonhazardous, and environmentally benign advantages (Anis *et al.*, 2008). There is a plethora of reports describing the role of nanoparticles to improve thermal degradation of nanocomposites (Pandey *et al.*, 2005; Leszczyńska *et al.*, 2007; Abd-Elrahman 2013; Mallakpour and Jarang 2015). Numerous research groups have focused on improving the thermal stability of PVA and PVA blends by the addition of fillers, lubricants, and crosslinking agents (Alexy *et al.*, 2002; Sreedhar *et al.*, 2005; Sreedhar *et al.*, 2006).

Zinc oxide (ZnO) nanoparticles are unique wide energy gap filler material that demonstrate highly attractive optical, electrical, and piezoelectric properties (Moezzi *et al.*, 2012). Furthermore, ZnO exhibits additional significant advantages such as relatively low toxicity, low-cost, and thermal and chemical stability.

The fundamental electronic transition onset of ZnO, at 3.37 eV, and a high room temperature excitonic stability (exciton binding-energy is ~60 meV) results in intense UV-blue luminescence (Sengupta *et al.*, 2011; Moezzi *et al.*, 2012).

The purpose of adding LiCl to nanocomposite blends is to determine its influence on the thermal degradation of the composite films, since the LiCl salt exhibits improvement in electrical conductivity when compared with other salts, such as $NaNO_3$, $CaCl_2$ and NaCl (Weast, 1989). Li^+ (1+ oxidation state) is expected to substitute Zn in ZnO, by utilizing vacancies of comparable size, since the ionic radii of Li (90 pm) and Zn (88 pm) ions are similar in size (Shannon, 1976). Additionally,

PVA/LiCl electrolytes have been used as electrochemical stabilizer pseudo-capacitors in vanadium oxide electrodes (Wang *et al.*, 2012). The addition of LiCl salt to PVA increases the hydrophilicity and vapor permeability of the hybrid material (Zhang *et al.*, 2008). Furthermore, the presence of the LiCl salt is a factor in the water sorption rate for PVA blends (Jiang *et al.*, 2016). However, this study focuses on studying the thermal degradation by kinetic analysis using Kissinger and Flynn-Wall-Osawa (FWO) models to measure the degradation activation energy (E_a) and to determine the most plausible degradation mechanism for pure PVA and PVA/ZnO/LiCl three-phase composite. This study benefits from optimizing the process conditions during the preparation of the three-phase blends, since thermal degradation is a result of the intrinsic processes of chemical reactions during film preparation.

MATERIALS AND METHODS

PVA (average mw. 30,000–70,000), zinc acetate dihydrate (Zn(CHCOO)•2H$_2$O), LiCl salt and sodium hydroxide (NaOH) were purchased from Sigma-Aldrich and used without any further purification. Distilled water is used having a resistivity of ~15 MΩ·cm.

For each sample, one gram of PVA powders was dissolved in 20 ml of distilled water and heated to 80 °C with magnetic stirring for 3 hrs. For the synthesis of ZnO nanoparticles, zinc acetate dihydrate powder (3 g) was dissolved in 40 ml of distilled water at ~40 °C. Thereafter, 4–6 NaOH pellets were added to the aqueous zinc acetate solution, under stirring, prior to heating for 4 hrs to form ZnO nanoparticles.

For PVA/ZnO nanocomposite samples, 0.25 mg of ZnO powder was dispersed in 5 ml of deionized (DI) water before mixing with the PVA solution. The mixture was ultrasonicated (5min) to get a homogenous mixture. Four containers comprising the clear and homogenous PVA/ZnO gel (fixed weight ratio of 5 wt.%), electrolyzed with varying weight ratios of LiCl (0, 3 and 6 wt.%) under magnetic stirring. The obtained nanocomposite solutions were poured into Petri dishes (diameter 5 cm). At room temperature, DI water was evaporated over a period of 24 hrs. The resultant films dried at 60 °C for 2 hrs. Film thickness was ~0.1 mm. The list of samples composition and code is presented in Table 1.

Table 1. Poly(vinyl alcohol) (PVA) blends with ZnO nanoparticles and LiCl salts.

Film No.	PVA	ZnO	LiCl
S1	1 g	-	-
S2	1 g	5%	0%
S3	1 g	5%	3%
S4	1 g	5%	6%

TA Q50 thermal gravimetrical analysis (TGA) instrument was used to measure the weight loss of the nanocomposite films as a function of temperature. The experiments were performed at various heating rates of 5, 10, 20, 30, 40, and 50 °C/min, under constant nitrogen purging (60 mL/min flow rate). For TGA analysis, all samples had approximately 12 mg and preheated to 200°C to avoid the overlapping of the TGA profile and remove the residual water.

Theoretical background

The kinetic study of thermal decomposition is categorized into differential and integral methods. The Coats-Redfern (Coats and Redfern, 1964; Ou *et al.*, 2010) and Flynn-Wall-Ozawa (FWO) (Ozawa, 1970; Wang *et al.*, 2009) models are attributed to the integral method, while the Kissinger model fits within the differential method (Kissinger, 1956 and 1957). In solid-state samples, the kinetic analysis is usually presented by the following empirical equation:

$$r = d\alpha/dt = K(T)f(\alpha) \tag{1}$$

where: α is the reacted fraction, $d\alpha/dt$ is the rate of conversion, $f(\alpha)$ is the kinetic model which usually related to a physical model describe the kinetic of the solid-state reaction. $K(T)$ is the rate constant, which

is temperature dependent, and is generally assumed to follow the Arrhenius equation:

$$K(T) = A \, exp(-E_a/RT) \tag{2}$$

where: A and E_a are the pre-exponential factor (mol^{-1}) and the activation energy (kJ/mol) of the kinetic process, respectively. R is the gas constant (8.314 J/(mol·K)) and T is the temperature (K).

Considering the heating rates, $\beta=dT/dt$, as a non-isothermal condition, the reaction rate equation can be written as (Li et al., 2009):

$$d\alpha/dt = A/\beta \, exp(E_a/RT) \, f(\alpha) \tag{3}$$

From a set of non-isothermal tests, Kissinger developed a method for estimation of activation energy of the reaction which given by;

$$ln\beta/T^2_{max} = ln(AR/E_a)-(E_a/R) \, 1/T_{max} \tag{4}$$

where: the temperature corresponding to DTGA (1st derivative of TGA curve) peak value.   By plotting $ln\beta/T^2_{max}$ versus $1000/T_{max}$, E_a and A can be calculated from the slope $(-E_a/R)$ and intercept $(ln(AR/E_a))$, of the fitted straight line, respectively.

From the integral method, Flynn-Wall-Ozawa (FWO) model is used directly to estimate the activation energy (E_a) using the following equation:

$$log\beta = log(A \, E_a/R \, g(\alpha)) - 2.315 - 0.4567 \, (E_a/RT) \tag{5}$$

where: $g(\alpha)$ is one of numerous integral formulas taken from the literature (thirteen of which are presented in Table 2). The activation energy at specific conversion (E_a) can be determined by plotting $log \, \beta$ against $1000/T$, since the value of $log(AE_a/Rg(\alpha))$ is approximately constant.

Table 2. Algebraic expressions for g(a) frequently used in the literature (Zhou et al. 2009).

Symbol	g(a)	Mechanism processes
	Sigmoidal curves	
A2	$[-ln(1-\alpha)]^2$	(Avrami equation (1))
A3	$[-ln(1-\alpha)]^3$	Nucleation and growth for different orders (Avrami equation (2)) (Avrami equation (3))
A4	$[-ln(1-\alpha)]^4$	
	Deceleration curves	
R1	α	Phase boundary controlled reaction (1D-movement)
R2	$2[1-ln(1-\alpha)^{1/2}]$	Phase boundary controlled reaction (contacting area)
R3	$3[1-ln(1-\alpha)^{1/3}]$	Phase boundary controlled reaction (contacting volume)
D1	α^2	1D diffusion
D2	$(1-\alpha) \, ln(1-\alpha) + \alpha$	2D diffusion (Vslensi equation)
D4	$[1-(2/3)\alpha] - (1-\alpha)^{2/3}$	3D diffusion (Ginstling-Brounshtein equation)
F1	$-ln(1-\alpha)$	Random nucleation with one nucleus on the individual particle
F2	$1/(1-\alpha)$	Random nucleation with two nuclei on the individual particle
F3	$1/(1-\alpha)^2$	Random nucleation with three nuclei on the individual particle
α = the degree of conversion.		

Another integral formula, referred as the Coats-Redfern (CR) model is described by the following equation:

$$ln \, (g(\alpha)/T^2) = ln \, (AR/\beta E_a) - (E_a/R) \, 1/T \tag{6}$$

The estimated values of E_a and A can be calculated for any chosen form of $g(\alpha)$ and fixed β.

In this study we rely on Kissinger and FWO models to estimate the apparent activation energy. Coats-Redfern model will be used with applying the predicted model, listed in Table 2, to estimate the apparent activation energy for the main decomposition reaction. Only these models that produce results close to the estimated values from Kissinger and FWO models will be discussed to

explain the decomposition mechanism for the main decomposition reaction of PVA nanocomposite samples.

RESULTS AND DISCUSSION

Thermogravimetric analysis curves (TGA) for pure PVA and its nanocomposite (PVA/ZnO) and its three phase (PVA/ZnO/LiCL) samples at different heating rates were

investigated in Figure 1. All samples were pre-heated up to 200°C before carrying out the TGA analysis to eliminate the residual water decomposition stage and reduce the probability of overlaps in the first derivative of the TGA curve (DTGA). Two distinguish decomposition stages are observed for pure and nanocomposite samples and for all heating rates.
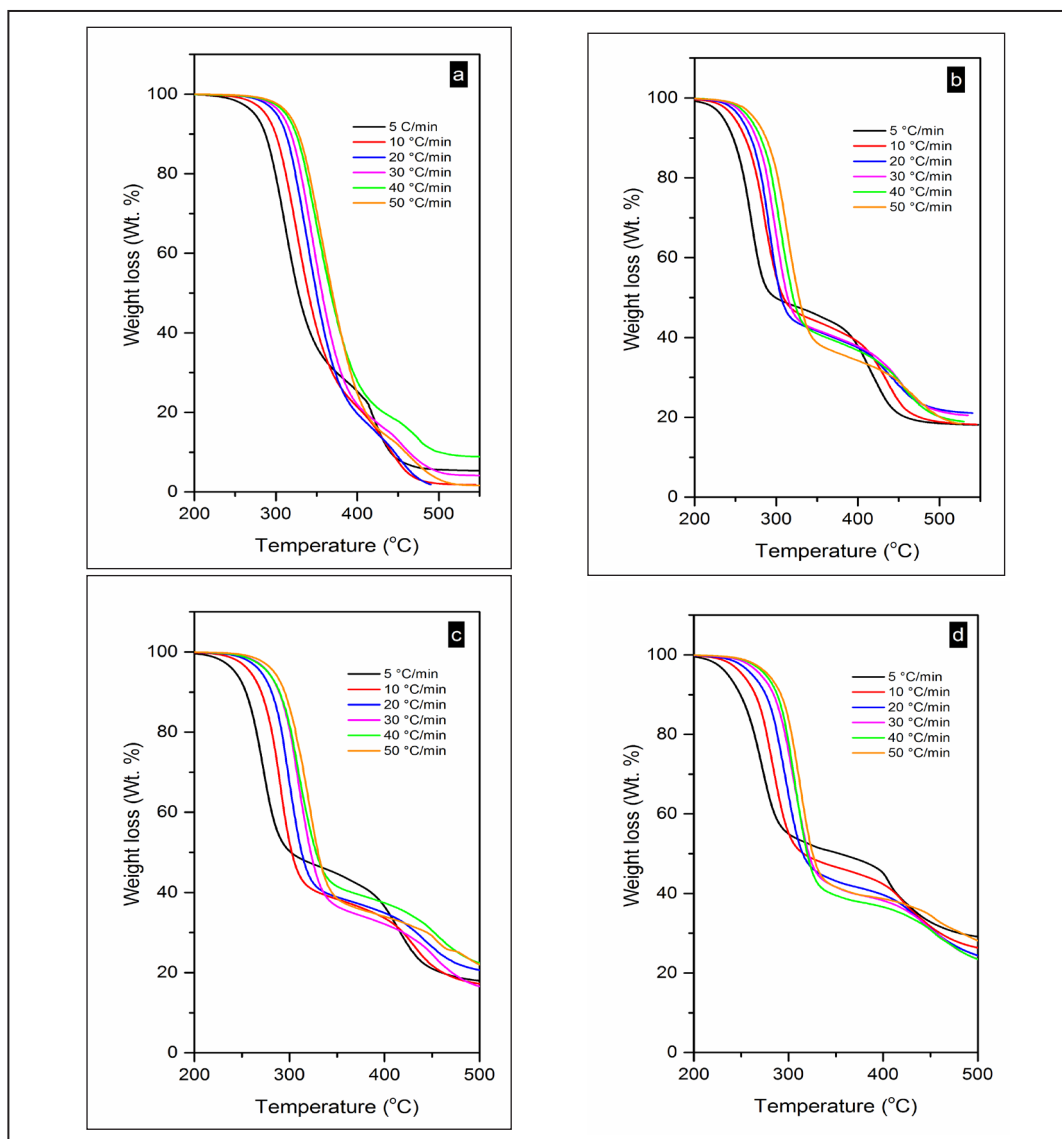

Figure 1. Thermogravimetric analysis (TGA) curves for different samples as a function of heating rate: a) pure poly(vinyl alcohol) (PVA) (S1), b) PVA/ZnO (S2), c) PVA/ZnO LiCl-3%, d) PVA/ZnO LiCl-6%.

For pure PVA (Figure **1**(a)), the first decomposition stage is attributed to the thermal degradation of the carboxylic acid side-chain, since PVA is not fully hydrolyzed. The second degradation stage corresponds to the degradation of main PVA chain

releasing alkynes (low-molecular weight) and conjugated polyenes (Peng *et al.* 2005). The first degradation stage was selected for kinetic studies.

Figure 2a and 2b shows the effect of ZnO nanoparticles (S1) and LiCl salt (S2 and S3)

on the thermal behavior of the samples at two different heating rates (10 and 20 °C/min). It is clear that the main effect is return to the addition of ZnO to the polymer matrix. The addition of LiCl salts has no effective change on the TGA profile curve. The addition of ZnO nanoparticles accelerate the degradation of main decomposition stage (first stage) of the polymer chains. The addition of ZnO nanoparticles will acts to separate the polymer chains and decrease agglomeration density. Besides, ZnO will cause partial degradation in the polymeric chains during preparation process and due to ultrasonication. Chains fracture will increase the number of chain ends (termination). These will facilitate the thermal decomposition of chains and reduce the thermal stability of the polymer.
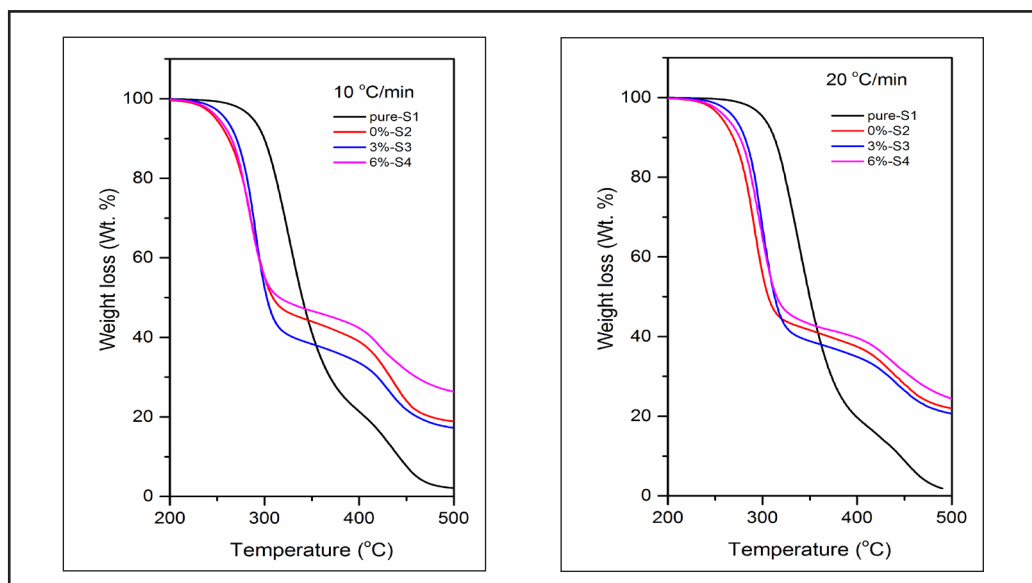

Figure 2. TGA curves for different samples at a heating rate of: a)10 °C/min, b) 20 °C/min.

For the second decomposition stage, the thermal stability was increased for the nanocomposite samples. This can be attributed to two factors. The first is the shortness of the chain length will decrease the probability of decomposition of the main chain double bond and polyene formation. The second, at high temperature stage, nanoparticles will be able to move to the composite surface (due to relatively low surface potential energy or surface tension). As a result, the accumulated ZnO nanoparticles act as insulating layers and barrier for mass transport, which delays both of polymer decomposition and the release of volatile products (as seen in figure 3).
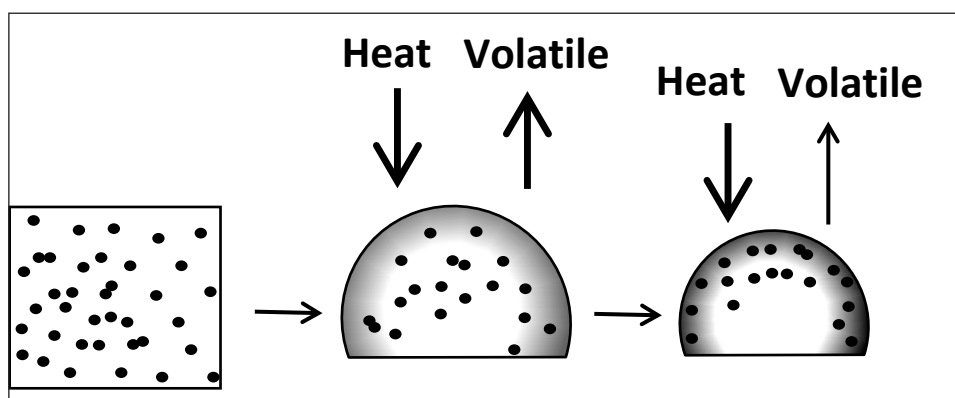

Figure 3. Illustration representing the ZnO nanoparticle distribution in PVA during combustion.

The thermal degradation mechanism, especially for nanocomposites, generally follows a complex reaction pathway and is dependent on α. Consequently, complex conversion mechanisms must be determined from experimental data. The Kissinger and FWO models were used to calculate the E_a of degradation for all samples. However, the Coats-Redfern model was used to determine the more plausible thermal degradation mechanisms in the presence of the ZnO nanoparticles and LiCl salt. Figure 4 shows the relation between plotting $ln\beta/T^2_{max}$ and $1000/T_{max}$ (Kissinger models) to estimate the apparent activation energies for all samples under test.
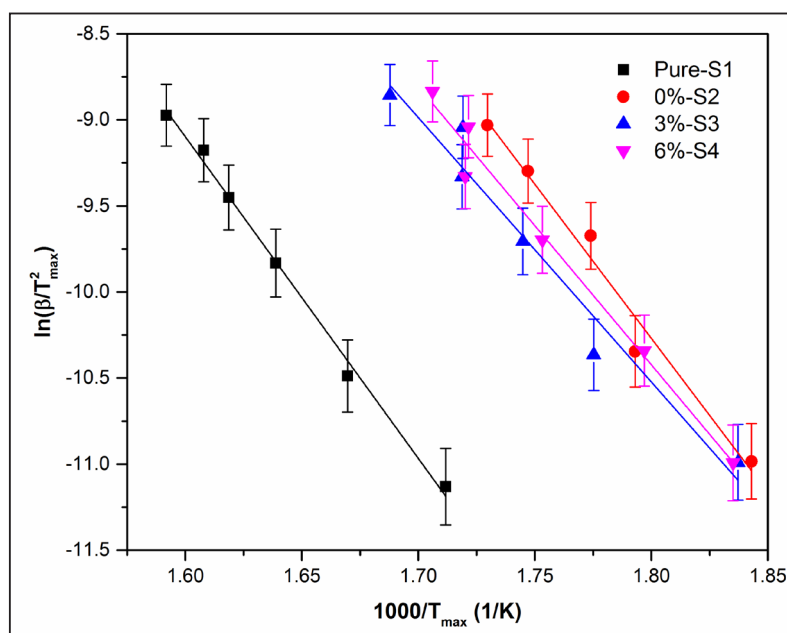

Figure 4. Kissinger models applied for sample data as a function of heating rate to calculate the degradation activation energy.

Pure PVA (S1) showed the highest apparent activation energy (E_a ~154.8 KJ mol^{-1}), which is comparable to the literature (Peng *et al.* 2006) and (Baraker and Lobo 2018). For both nanocomposite and nanocomposite electrolyte sample, the apparent activation energy dropped steadily in to 148.8 KJ mol^{-1} for PVA/ZnO and 127.2 and 133.8 KJ mol^{-1} for S3 and S4 nanocomposite electrolyte samples respectively. These results confirm the reduction of thermal stability of the samples. Table 3 illustrates the values of the apparent activation energy for pure, nanocomposite and electrolyte nanocomposite samples predicted by Kissinger model. Beside the value of R^2 which indicates the goodness of fit measure for the linear regression.

Table 3. Activation energy from Kissinger model.

Pure-S1		0%-S2		3%-S3		6%-S4	
E(kJmol^{-1})	R-square	E(kJmol^{-1})	R-square	E(kJmol^{-1})	R-square	E(kJmol^{-1})	R-square
154.8	0.994	148.8	0.968	127.2	0.954	133.8	0.978

Table 4 illustrates the values of the apparent activation energy for pure, nanocomposite and electrolyte nanocomposite samples predicted by using FWO model. The calculated activation energies from both the Kissinger and FWO models, are close to each other.

Table 4. Activation energy from FWO model at heating rates (beta=5, 10, 20, 30, 40, 50).

A conversion	Pure-S1		0%-S2		3%-S3		6%-S4	
	E(kJmol⁻¹)	R-square	E(kJmol⁻¹)	R-square	E(kJmol⁻¹)	R-square	E(kJmol⁻¹)	R-square
0.7	145.6	0.987	137.4	0.945	134.8	0.988	146.2	0.993
0.65	144.4	0.991	137.2	0.95	133	0.986	142.7	0.993
0.6	145.2	0.99	137.2	0.955	131.4	0.983	140.2	0.993
0.55	144.2	0.993	137	0.957	130.2	0.980	138.4	0.994
0.5	145.4	0.993	137	0.954	129.5	0.978	136.1	0.993
0.4	143.9	0.995	135.6	0.965	127.5	0.974	130.4	0.993

A number of recommended models (listed in table 2), which assume different mechanisms of thermal degradation of mater, have been used to estimate the values of the apparent activation energy (E_a) for pure, nanocomposite and electrolyte nanocomposite samples (see Tables 5 to 7).

Table 5. Activation energy from Mechanism (D1) of Coats Redfern model at (α=0.7, 0.65, 0.6, 0.55, 0.5, 0.4).

Rate (ºC/min)	Pure-S1		0%-S2		3%-S3		6%-S4	
	E(kJmol⁻¹)	R-square	E(kJmol⁻¹)	R-square	E(kJmol⁻¹)	R-square	E(kJmol⁻¹)	R-square
5	148.8	0.98	200.2	0.992	195.7	0.980	174.1	0.991
10	140.3	0.965	189.6	0.988	240.8	0.988	208.4	0.987
20	151.6	0.979	230.8	0.995	242.0	0.979	217.1	0.988
30	158.2	0.971	218.6	0.989	231.0	0.987	214.6	0.994
40	140.9	0.985	205.1	0.990	209.2	0.978	247.6	0.986
50	148	0.981	205.5	0.990	219.2	0.994	249.5	0.99

Table 6. Activation energy from Mechanism (F1) of Coats Redfern model at (α=0.7, 0.65, 0.6, 0.55, 0.5, 0.4).

Rate (ºC/min)	Pure-S1		0%-S2		3%-S3		6%-S4	
	E(kJmol⁻¹)	R-square	E(kJmol⁻¹)	R-square	E(kJmol⁻¹)	R-square	E(kJmol⁻¹)	R-square
5	111.9	0.995	151.0	0.999	148.0	0.994	131.2	0.999
10	105.4	0.986	143.3	0.999	182.2	0.998	157.6	0.998
20	114.2	0.995	174.8	1.000	183.3	0.994	164.2	0.998
30	119.2	0.99	165.4	0.999	174.6	0.998	162.1	1
40	105.7	0.996	154.9	0.999	158.1	0.993	187.6	0.998
50	111.6	0.995	154.9	0.999	164.9	0.999	188.8	0.999

Table 7. Activation energy from Mechanism (F2) of Coats Redfern model at (α=0.7, 0.65, 0.6, 0.55, 0.5, 0.4).

Rate (ºC/min)	Pure-S1		0%-S2		3%-S3		6%-S4	
	E(kJmol⁻¹)	R-square	E(kJmol⁻¹)	R-square	E(kJmol⁻¹)	R-square	E(kJmol⁻¹)	R-square
5	88.7	0.991	119.8	0.978	118.1	0.992	104.1	0.979
10	83.7	0.996	114.3	0.984	145.1	0.985	125.6	0.984
20	91.2	0.989	139.5	0.973	146.5	0.993	130.8	0.983
30	95	0.991	131.9	0.985	138.9	0.987	129	0.974
40	83.8	0.982	123.3	0.981	126.0	0.993	149.9	0.986
50	89.3	0.988	122.7	0.983	130.1	0.974	150.6	0.981

The calculated values were compared with that of the average values from Kissinger and FWO models (Table 8) to suggest the optimum degradation mechanism model relating to each sample. From this comparison, pure PVA degradation mechanism was suggested to obey D1 model which involves one-dimensional diffusion process. The other samples (two and three phase samples) are closed to obey F2 model which involve random nucleation with two nuclei on the individual particle. PVA/ZnO nanocomposite sample (S2) tends to obey F1 model more than F2 model, but both

rely the random nucleation process. This result is highly satisfactory since the two and three phase samples are more complex than pure PVA. The nature of each point inside the complex system may differ according to its status. For examples, the chains confined within aggregation of ZnO will have a different thermal behavior than the chains just attached to ZnO nanoparticles or for chains surrounded by another chains (agglomeration). Conversely, the presence of salts had negligible influence on the degradation mechanism.

Table 8. Summary of the activation energy values of all samples and the average values of Kissinger and FWO models.

	Pure S1	S2	S3	S4
Kissinger model	154.80	148.80	127.20	133.80
FWO model	144.78	136.90	131.07	139.00
Average Kissinger and FWO models	149.79	142.85	129.14	136.4
D1 (1D diffusion)	147.97	208.30	222.98	218.55
F1 (Random nucleation with one nucleus on the individual particle)	111.33	157.38	168.52	165.25
F2 (Random nucleation with two nuclei on the individual particle)	88.62	125.25	134.12	131.67

CONCLUSION
Nanocomposite of polyvinyl alcohol ZnO loaded with different concentration of LiCl salts were prepared through casting technique. Thermal degradation and stability were investigated through thermal gravimetrical analysis (TGA). The TGA results showed that the addition of ZnO reduce the thermal stability of the composite compared with pure PVA sample. The addition of LiCl salt did not show any change in thermal stability, especially for the main reaction stage. The thermal kinetic analysis for all samples was investigated to identify the decomposition mechanism in the two phase and three phase samples. Kissinger, FWO and Coats Redfern model were tested to calculate the apparent activation energy for all samples. Both Kissinger and FWO showed close activation energies' value which was

considered to describe quantitatively the degradation mechanisms for all samples. Pure PVA sample went to a mechanism (D1) of one-dimensional diffusion; however, the reset of samples went to a mechanism (F1) and (F2) of random nucleation with one and two nucleus on the individual particle, respectively.

REFERENCES
Abd-Elrahman, M. I. 2013. Enhancement of thermal stability and degradation kinetics study of poly(vinyl alcohol)/zinc oxide nanoparticles composite. Journal of Thermoplastic Composite Materials. 27: 160–166.

Alexy, P., Káchová, D., Kršiak, M., Bakoš D., and Šimková, B. 2002. Poly(vinyl alcohol) stabilisation in thermoplastic processing. Polymer Degradation and Stability. 78: 413–421.

Anis, A., Banthia, A. K., and Bandyopadhyay, S. 2008. Synthesis and characterization of polyvinyl alcohol copolymer/ phosphomolybdic acid-based crosslinked composite polymer electrolyte membranes. Journal of Power Sources. 179: 69–80.

Baraker, B. M., and B. Lobo. 2018. Multistage thermal decomposition in films of cadmium chloride-doped PVA–PVP polymeric blend. Journal of Thermal Analysis and Calorimetry. 134: 865-878

Coats, A. W., and Redfern, J. P. 1964. Kinetic Parameters from Thermogravimetric Data. Nature. 201: 68–69.

Godovsky, D. Y. 2000. Device Applications of Polymer-Nanocomposites. pp 163–205. Biopolymers· PVA Hydrogels, Anionic Polymerisation Nanocomposites. Springer Berlin Heidelberg, Berlin, Heidelberg.

Jiang, X., Li, H., Luo, Y., Zhao, Y., and Hou, L. 2016. Studies of the plasticizing effect of different hydrophilic inorganic salts on starch/ poly (vinyl alcohol) films. International Journal of Biological Macromolecules. 82: 223–230.

Jin, Y., Diniz da Costa, J. C., and Lu, G. Q. 2007. Proton conductive composite membrane of phosphosilicate and polyvinyl alcohol. Solid State Ionics 178: 937–942.

Kissinger, H. E. 1956. Variation of peak temperature with heating rate in different rate in differential thermal analysis. Journal of Research of the National Bureau of Standards. 57: 217–221.

Kissinger, H. E. 1957. Reaction kinetics in differential thermal analysis. Analytical Chemistry. 29: 1702–1706.

Krumova, M., López, D., Benavente, R., Mijangos, C., and Pereña, J. M. 2000. Effect of crosslinking on the mechanical and thermal properties of poly(vinyl alcohol). Polymer. 41: 9265–9272.

Leszczyńska, A., Njuguna, J., Pielichowski, K., and Banerjee, J. R. 2007. Polymer/ montmorillonite nanocomposites with improved thermal properties: Part I. Factors influencing thermal stability and mechanisms of thermal stability improvement. Thermochimica Acta. 453: 75–96.

Li, X., Wu, Y., Gu, D., and Gan, F. 2009. Thermal decomposition kinetics of nickel(II) and cobalt(II) azo barbituric acid complexes. Thermochimica Acta. 493: 85–89.

Mallakpour, S., and Jarang, N. 2015. Mechanical, thermal and optical properties of nanocomposite films prepared by solution mixing of poly(vinyl alcohol) with titania nanoparticles modified with citric acid and vitamin C. Journal of Plastic Film & Sheeting. 32: 293–316.

Moezzi, A., McDonagh, A. M., and Cortie, M. B. 2012. Zinc oxide particles: Synthesis, properties and applications. Chemical Engineering Journal. 185–186: 1–22.

Ou, C.-Y., Zhang, C.-H., Li, S.-D., Yang, L., Dong, J.-J., Mo, X.-L., and Zeng, M.-T. 2010. Thermal degradation kinetics of chitosan-cobalt complex as studied by thermogravimetric analysis. Carbohydrate Polymers. 82: 1284–1289.

Ozawa, T. 1970. Kinetic analysis of derivative curves in thermal analysis. Journal of Thermal Analysis. 2: 301–324.

Pandey, J. K., Raghunatha Reddy, K., Pratheep Kumar, A., and Singh, R. P. 2005. An overview on the degradability of polymer nanocomposites. Polymer Degradation and Stability. 88: 234–250.

Peng, Z., Kong, L., and Li, S.-D. 2005. Thermal properties and morphology of poly(vinyl alcohol)/silica nanocomposite prepared with self-assembled monolayer techniques. Journal of Applied Polymer Science. 96: 1436_1442.

Peng, Z., Kong, L. X., Li, S.-D., and Spiridonov, P. 2006. Poly(vinyl alcohol) /silica nanocomposites: Morphology and thermal degradation kinetics. Journal of Nanoscience and Nanotechnology. 6: 3934–3938.

Sengupta, J., Sahoo, R. K., Bardhan, K. K., and Mukherjee, C. D. 2011. Influence of annealing temperature on the structural, topographical and optical properties of sol-gel derived ZnO thin films. Materials Letters. 65: 2572–2574.

Shannon, R. 1976. Revised effective ionic radii and systematic studies of interatomic distances in halides and chalcogenides. Acta Crystallographica Section A. 32: 751–767.

Sreedhar, B., Sairam, M., Chattopadhyay, D. K., Rathnam, P. A. S., and Rao, D. V. M. 2005. Thermal, mechanical, and surface characterization of starch-poly(vinyl alcohol) blends and borax-crosslinked films. Journal of Applied Polymer Science. 96: 1313–1322.

Sreedhar, B., Chattopadhyay, D. K., Karunakar, M. S. H., and Sastry, A. R. K. 2006. Thermal and surface characterization of plasticized starch polyvinyl alcohol blends crosslinked with epichlorohydrin. Journal of Applied Polymer Science. 101: 25–34.

Wang, G., Lu, X., Ling, Y., Zhai, T., Wang, H., Tong, Y., and Li, Y. 2012. LiCl/PVA gel electrolyte stabilizes vanadium oxide nanowire electrodes for pseudocapacitors. ACS Nano. 6: 10296–10302.

Wang, Q. F., Wang, L., Zhang, X. W., and Mi, Z. T. 2009. Thermal stability and kinetic of decomposition of nitrated HTPB. Journal of Hazardous Materials. 172: 1659–1664.

Weast, R. C. 1989. CRC Handbook of Chemistry and Physics. 70th edition. CRC Press, Boca Raton, FL.

Zhang, L.-Z., Wang, Y.-Y., Wang, C.-L., and Xiang, H. 2008. Synthesis and characterization of a PVA/LiCl blend membrane for air dehumidification. Journal of Membrane Science. 308: 198–206.

Zhou, X. Y., Jia, D. M., Cui, Y. F., and Xie, D. 2009. Kinetics analysis of thermal degradation reaction of PVA and PVA/starch blends. Journal of Reinforced Plastics and Composites. 28: 2771–2780.

الانحلال الحراري بواسطة التحليل الحركي لمادة ممتزجة من ثلاثية الطور (PVA / ZnO / LiCl)

عبد الله فيصل محمد النعيم

قسم الفيزياء، كلية العلوم، جامعة الملك فيصل

الأحساء، المملكة العربية السعودية

الملخص

تمت دراسة حركية الانحلال الحراري للبولي (فينيل كحول) (PVA) ومزيجها عند نسبة وزن مختلفة من الجسيمات النانوية ZnO و LiCl كمحرر تشابك لسلسلة الـ PVA بواسطة القياس الحراري (TGA) وقد خضعت البيانات المتحصل عليها لتحليل حراري غير متساوي التحليل الحراري للعينات عند معدلات تسخين 5 و 10 و 20 و 30 و 40 و 50 درجة مئوية\دقيقة، تم حساب طاقة التنشيط من التحلل الحراري وآلياتها باستخدام نماذج كيسنجر، فلين، وول، أوزاوا وكوت ريدفرين. بشكل عام، أظهرت جميع النماذج موثوقيتها لوصف الانحلال الحراري للعينات. تظهر النتائج انخفاض الثبات (الاستقرار) الحراري PVA في وجود الجسيمات النانوية ZnO، أيضا، الجسيمات النانوية ZnO تُغيِّر آلية التحلل من انتشار في بعد واحد إلى التنوي العشوائي مع واحد أو اثنين من النواة على الجسيمات الفردية. ومع ذلك، يظهر الملح LiCl آثارًا طفيفة في قيم طاقات التنشيط والتأثير في منحنيات TGA.

الكلمات المفتاحية: بولي (فينيل الكحول)، تدهور (التحلل) حراري، جسيمات متناهية الصغر، الاستقرار الحراري، ثلاثي الطور، المعبئات.